ELSEVIER

Journal of Chromatography A, 971 (2002) 207–215

JOURNAL OF CHROMATOGRAPHY A

www.elsevier.com/locate/chroma

Prediction of electrophoretic mobilities of alkyl- and alkenylpyridines in capillary electrophoresis using artificial neural networks

M. Jalali-Heravi*, Z. Garkani-Nejad

Department of Chemistry, Sharif University of Technology, P.O. Box 11365-9516, Tehran, Iran

Received 2 January 2002; received in revised form 8 July 2002; accepted 11 July 2002

Abstract

The electrophoretic mobilities of 31 isomeric alkyl- and alkenylpyridines in capillary electrophoresis were predicted using an artificial neural network (ANN). The multiple linear regression (MLR) technique was used to select the descriptors as inputs for the artificial neural network. The neural network is a fully connected back-propagation model with a 3-6-1 architecture. The results obtained using the neural network were compared with those obtained using the MLR technique. Standard error of training and standard error of prediction were 6.28 and 5.11%, respectively, for the MLR model and 1.03 and 1.20%, respectively, for the ANN model. Two geometric parameters and one electronic descriptor that were used as inputs in the ANN are able to distinguish between the isomers.

Keywords: Electrophoretic mobility; Neural networks, artificial; Regression analysis; Molecular descriptors; Structure–activity relationships; Alkylpyridines; Alkenylpyridines; Pyridines

1. Introduction

Capillary electrophoresis (CE) shows many advantages over conventional separation techniques like gas chromatography (GC) or HPLC methods. This method offers the advantages of high resolution and separation efficiency and good reproducibility. In CE, analytes are separated due to their different velocities under the influence of an electric field. The analytes reach a steady-state velocity that can be expressed independently of the field strength as the electrophoretic mobility (μ_e). The electrophoretic mobility (μ_e) of an analyte at a given ionic strength can be determined using Eq. (1):

$$\mu_e = \frac{L_d}{E} \cdot \left(\frac{1}{t_m} - \frac{1}{t_{eof}} \right) \quad (1)$$

where L_d is the length from inlet to the detector, E is the applied potential, t_m is the observed analyte migration time, and t_{eof} is the migration time of a neutral marker.

The search for optimal separation conditions is sometimes time consuming and tedious. Therefore,

*Corresponding author. Tel.: +98-21-600-5718; fax: +98-21-601-2983.

E-mail address: jalali@sharif.edu (M. Jalali-Heravi).

0021-9673/02/$ – see front matter
PII: S0021-9673(02)01043-9

development of theoretical models for estimating electrophoretic mobility seems to be useful.

The relationship between the structures of a range of molecules and their mobilities has been examined by Kaliszan et al. [1]. As a quantitative structure–retention relationship, they suggested that a close correlation could be obtained with the ionic radius for a series of lanthanide cations. In a study by Liang et al., it is indicated that the migration rates of a series of flavonoids in a buffered CE system are related to a combination of the molecular connectivity indexes [2]. Also, Lukkari and Yang have studied the relation between the connectivity indexes and the MEKC separations of β-blockers and corticosteroids [3,4].

The use of artificial neural networks (ANNs) in chemistry has grown substantially [5,6]. There are several reports on the use of neural networks in the modeling of retention behavior and optimization of conditions in micellar liquid chromatography [7,8]. ANNs have been applied by several groups in quantitative structure–activity relationship (QSAR) studies [9–12]. In a previous work, we have studied the relation between electrophoretic mobility of some cationic and anionic sulfonamides with the structural parameters [13]. In that work, surface area of cationic and anionic species, heat of formation and positive partial charge on the anions were related with the electrophoretic mobility. In the present work, the usefulness of artificial neural networks for modeling of the electrophoretic mobility of alkyl- and alkenylpyridines is investigated and is compared to the established methods like linear regression techniques.

2. Theory

Artificial neural networks are mathematical systems that simulate biological neural networks. They consist of processing elements (neurons) organized in layers. The neural network used in this work is of the back-propagation neural network (BNN) type [14–19]. A typical feed-forward neural network with back-propagation has three layers: the input, the hidden, and the output layers. The activation of a neuron is defined as the sum of the weighted input signals to that neuron:

$$\mathrm{Net}_j = \sum_i W_{ij} X_i + \mathrm{bias}_j \quad (2)$$

where W_{ij} is the weight-connection to neuron j in the actual layer from neuron i in the previous layer and bias_j is the bias of neuron j. The Net_j of the weighted inputs is transformed with a transfer function, which is used to get to the output level. Several functions can be used for this purpose, but the ''sigmoid function'' is mostly applied. This function is as follows:

$$y_j = \frac{1}{1 + e^{-\mathrm{Net}_j}} \quad (3)$$

where y_j is output of the neuron j. The BP network learns by adjusting its weights according to the error (E) (Eq. (4)). The goal of training of a network is to change the weights between the layers in a direction that minimizes the error, E:

$$E = \frac{1}{2} \sum_p \sum_k (y_{p_k} - t_{p_k})^2 \quad (4)$$

The error E of a network is defined as the squared differences between the target values t and the outputs y of the output neurons summed over p training patterns and k output nodes.

In the present work, the main goal was development of an ANN for modeling of the electrophoretic mobilities of a series of alkyl- and alkenylpyridines. A linear regression model was also developed and its results were compared with the calculated ANN electrophoretic mobilities. This comparison will clarify the nonlinear characteristics of the electrophoretic mobility of different pyridines studied in this work.

3. Experimental

3.1. Data set

The electrophoretic mobilities of a series of isomeric alkyl- and alkenylpyridines consisting of 31 molecules was taken from Ref. [20] as the data set. In this reference, fused-silica capillaries of 50 and 75 μm internal diameter (I.D.) (Beckman) were used with an inlet to outlet length of 57 cm and an inlet to detector length of 50 cm. The electrophoretic mobilities of substituted pyridines have been determined

at pH 2.5 in a lithium phosphate buffer. Under these conditions, the studied compounds will effectively bear a full positive charge. The relationship between the structure and electrophoretic mobility of these compounds has been considered.

In the present work, this data set was randomly divided into two groups, a training set consisting of 22 compounds and a prediction set that includes nine compounds (Table 1). The training set was used for the generation of the network and the prediction set was used to evaluate the generated network. The electrophoretic mobility of studied compounds ranged from 2.602×10^{-4} ($cm^2\ V^{-1}\ s^{-1}$) for *E*-2-(3-pentenyl)pyridine to 4.176×10^{-4} ($cm^2\ V^{-1}\ s^{-1}$) for the pyridine.

3.2. Descriptor generation

In the present work the descriptors are numerical parameters that relate electrophoretic mobility (μ_e) of the molecules with their structures. These parameters include topological, geometric and electronic

Table 1
Experimental, ANN and MLR calculated values of electrophoretic mobilities together with the values of the descriptors appearing in the model for the training and prediction sets

No.	Compound	Descriptors[a]			Mobility[b]		
		DIMO	$(RVDW)^{-1}$	MO_x	μ_{ANN}	μ_{MLR}	μ_{EXP}
Training set							
1	Pyridine	1.974	0.368	0.199	4.172	4.034	4.176
2	2-Methylpyridine	1.723	0.347	0.187	3.576	3.593	3.581
3	4-Methylpyridine	2.324	0.347	0.192	3.746	3.720	3.722
4	2-Ethylpyridine	1.679	0.329	0.154	3.164	3.251	3.222
5	4-Ethylpyridine	2.401	0.330	0.165	3.400	3.406	3.397
6	2,3-Dimethylpyridine	1.880	0.330	0.105	3.208	3.243	3.236
7	2,5-Dimethylpyridine	1.853	0.330	0.180	3.226	3.317	3.236
8	2,6-Dimethylpyridine	1.479	0.329	0.120	3.129	3.173	3.168
9	3,4-Dimethylpyridine	2.479	0.330	0.108	3.293	3.359	3.349
10	3,5-Dimethylpyridine	2.235	0.330	0.122	3.306	3.329	3.285
11	2-Propylpyridine	1.640	0.315	0.150	2.900	2.988	2.923
12	4-Isopropylpyridine	2.344	0.315	0.115	3.082	3.089	3.059
13	3-Ethyl-4-methylpyridine	2.437	0.316	0.085	3.036	3.077	3.071
14	6-Ethyl-2-methylpyridine	1.436	0.315	0.098	2.898	2.893	2.904
15	2,4,6-Trimethylpyridine	1.819	0.316	0.061	2.840	2.933	2.849
16	3-Butylpyridine	2.120	0.303	0.124	2.843	2.839	2.848
17	2-*tert*.-Butylpyridine	1.553	0.303	0.086	2.744	2.696	2.748
18	2-Pentylpyridine	1.708	0.292	0.120	2.544	2.573	2.534
19	2-(1-Ethylpropyl)pyridine	1.686	0.293	0.069	2.547	2.514	2.521
20	2,4,6-Tri-*tert*.-butylpyridine	1.558	0.251	0.016	1.814	1.699	1.809
21	4-Vinylpyridine	2.247	0.335	0.179	3.516	3.488	3.597
22	*E*-2-(3-Pentenyl)pyridine	1.583	0.296	0.137	2.601	2.624	2.602
Prediction set							
23	3-Methylpyridine	1.102	0.347	0.186	3.736	3.671	3.721
24	3-Ethylpyridine	2.092	0.330	0.154	3.358	3.333	3.366
25	2,4-Dimethylpyridine	2.068	0.330	0.123	3.288	3.293	3.196
26	4-Propylpyridine	2.351	0.315	0.152	3.138	3.129	3.097
27	5-Ethyl-2-methylpyridine	1.840	0.315	0.148	2.992	3.029	2.976
28	4-*tert*.-Butylpyridine	2.429	0.304	0.087	2.815	2.870	2.828
29	2-Hexylpyridine	1.670	0.283	0.105	2.375	2.389	2.391
30	2-Vinylpyridine	1.496	0.335	0.175	3.377	3.337	3.388
31	*Z*-2-(3-Pentenyl)pyridine	1.650	0.296	0.101	2.624	2.593	2.640

[a] Definitions of the descriptors are given in the text.
[b] μ is mobility in $10^4\ cm^2\ V^{-1}\ s^{-1}$.

descriptors [21]. A total of 54 descriptors were calculated for each molecule of the data set. These descriptors are listed in Table 2. In order to calculate geometric and electronic descriptors, the three-dimensional structures of molecules were optimized using the AM1 Hamiltonian implemented in the semiempirical molecular orbital program of MOPAC [22] and Hyperchem package [23].

3.3. Regression analysis

A stepwise multiple linear regression procedure was used for model generation. From pairs of variables with $R > 0.90$, only one of them was used in modeling. By using this criterion, 27 out of 54 original descriptors were eliminated and the remaining descriptors were used to generate the models using the SPSS/PC software package [24]. The stepwise procedure was used for selection of descriptors. This method combines forward and backward procedures. Due to the complexity of intercorrelations, the variance explained by certain variables will change when new variables enter the equation. Sometimes a variable that qualified to enter loses some of its predictive validity when other variables enter. If this takes place, the stepwise method will remove the weakened variable. A final set of selected equations was then tested for stability and validity through a variety of statistical methods. The choice of which equation to consider further was made by using four criteria: multiple correlation coefficient (R), standard error (SE), F statistic and the number of descriptors in the model. The best multiple linear regression (MLR) model is one that has high R and F values, low standard error, least number of descriptors, and high ability for prediction. The best model selected in this work is presented in Table 3.

3.4. Neural network generation

The ANN program was written in FORTRAN 77 in our laboratory. The network was generated using the descriptors appearing in the MLR model as inputs. A three-layer network with a sigmoidal transfer function was designed. The initial weights were randomly selected from a uniform distribution between -1 and $+1$. Before training, the input and output values were normalized between 0.1 and 0.9. The number of neurons in the hidden layer, learning rate and momentum were optimized. The standard error of training (SET) and standard error of prediction (SEP) at the beginning of overtraining were plotted versus the number of neurons in the hidden layer at an arbitrary learning rate and momentum (Fig. 1a). The standard error (SE) for the training or prediction sets was calculated as follows:

$$\mathrm{SE} = \sqrt{\frac{\sum_{i=1}^{n}(t_i - y_i)^2}{n}} \tag{5}$$

where t_i and y_i are the target and calculated output values, respectively, and n indicates the number of training or prediction patterns.

The number of neurons in the hidden layer at the minimum of this curve was selected as the optimum number. Then, learning rate and momentum was optimized in a similar way (Fig. 1b and c). It can be seen from Fig. 1 that the optimum number of nodes in the hidden layer is 6 and the optimum values of the learning rate and momentum are 0.8 and 0.9, respectively. In addition, it should be noted that the number of input nodes is 3, that is equal to the number of descriptors appearing in the MLR model and the number of output nodes is 1.

4. Results and discussion

The experimental and calculated values of the electrophoretic mobilities using MLR and ANN methods for the alkyl- and alkenylpyridines studied in this work together with the values of the descriptors appearing in the selected MLR model are given in Table 1.

4.1. Multiple regression analysis

The MLR technique was performed on the molecules of the training set that are shown in Table 1. After regression analysis a few suitable models were obtained and among them, the best model was selected and presented in Table 3. Three descriptors have appeared in this model. These descriptors consist of reciprocal of van der Waals radius of the

Table 2
Descriptors studied in this work

No.	Descriptor	Notation
1	No. of atoms	NOATM
2	No. of carbon atoms	NOC
3	No. of hydrogen atoms	NOH
4	No. of non-hydrogen atoms	NNHA
5	No. of bonds	NOB
6	No. of non-hydrogen bonds	NNHB
7	Relative no. of carbon atoms	RNCA
8	Relative no. of hydrogen atoms	RNHA
9	Relative mass of carbon atoms	RMCA
10	Relative mass of hydrogen atoms	RMHA
11	Winer number	W
12	Balaban index	B
13	Zero-order valence connectivity index	$^{0}\chi$v
14	Path one connectivity index	$^{1}\chi$p
15	Path two connectivity index	$^{2}\chi$p
16	Path three connectivity index	$^{3}\chi$p
17	Cluster three connectivity index	$^{3}\chi$c
18	Path four connectivity index	$^{4}\chi$p
19	Cluster four connectivity index	$^{4}\chi$c
20	van der Waals volume	VOL
21	Surface area	SA
22	Shape factor	SHFAC
23	van der Waals radius	RVDW
24	Shadow area in x–y plane	SHDWxy
25	Shadow area in x–z plane	SHDWxz
26	Shadow area in y–z plane	SHDWyz
27	Standardized shadow area in x–y plane	SSxy
28	Standardized shadow area in x–z plane	SSxz
29	Standardized shadow area in y–z plane	SSyz
30	Distance between center of mass and center of charge	RI
31	Inverse of van der Waals radius	$(\mathrm{RVDW})^{-1}$
32	Inverse of distance between center of mass and center of charge	$(\mathrm{RI})^{-1}$
33	Principal moment of inertia around x axis	MO_x
34	Principal moment of inertia around y axis	MO_y
35	Principal moment of inertia around z axis	MO_z
36	Relative of MO_x to MO_y	MO_{xy}
37	Relative of MO_x to MO_z	MO_{xz}
38	Relative of MO_y to MO_z	MO_{yz}
39	Molecular density	MD
40	Molecular weight	MW
41	No. of primary carbons (sp^3)	NCP
42	Total energy	TOTEN
43	Electronic energy	ELEN
44	Core–core repulsion	CCR
45	Electronic density	ELDEN
46	Most positive partial charge	PPCH
47	Most negative partial charge	NPCH
48	Heat of formation	ΔH
49	Ionization potential	IP
50	Dipole moment	DIMO
51	Polarizability	POL
52	Square of polarizability	$(\mathrm{POL})^2$
53	Energy of highest occupied molecular orbital	HOMO
54	Energy of lowest unoccupied molecular orbital	LUMO

Table 3
Selected model of multiple linear regression[a]

Descriptor	Notation	Coefficient	Mean effect
Reciprocal of Van der Waals radius	$(RVDW)^{-1}$	17.356 (±0.955)	5.537
Dipole moment	DIMO	0.192 (±0.043)	0.368
Principal moment of inertia around *x* axis	MO_x	1.150 (±0.468)	0.145
Constant		−2.966 (±0.248)	

[a] Statistics of the model: $n=22$, $R=0.993$, SE = 0.062 and $F=429$.

molecules $(RVDW)^{-1}$ and principal moment of inertia of the molecules around the *x* axis (MO_x) that are geometric, and dipole moment of the molecules (DIMO) that is an electronic descriptor. Also, in order to obtain the extent of contributions of each descriptor in the electrophoretic mobility, the mean effect of each parameter was calculated and given in Table 3. The mean effect of a descriptor is the product of its mean and the regression coefficient in the MLR model. The parameter of $(RVDW)^{-1}$ relates the electrophoretic mobility with the structure and size of the molecules. For calculation of this parameter, the algorithm given by Stouch and Jurs was used and its program was written in FORTRAN 77 in our laboratory [25]. It can be seen from Table 3 that $(RVDW)^{-1}$ shows a larger mean effect than DIMO and MO_x. The mean effect and coefficient of this parameter in the MLR model indicates that electrophoretic mobility decreases as the size of the molecules increases. It is generally assumed that electrophoretic mobility is given by $\mu_e = q/6\pi\eta r$, where r is the hydrodynamic radius of the analyte [26]. On the other hand, Edward and Waldron have proposed the semiempirical relationship of $\mu_e = 1.14\times10^{-3}Zf/f^0 r_w$, where r_w is the van der Waals radius of the species and Z is the charge of the ion and f/f^0 is the frictional ratio for nonspherical molecules [27]. The presence of this descriptor in the model reveals the agreement between the experimental and theoretical studies. In capillary electrophoresis, analytes are separated due to the differences in their velocities under the influence of the electric field and therefore the electronic parameters such as DIMO may have an important role in this technique. The appearance of dipole moment in this model is particularly useful for distinguishing between the isomers, specially *Z* and *E* isomers. The coefficient of this parameter in the model indicates that with increasing of this parameter, the motion of cations toward the cathode and their electrophoretic mobilities increase. This parameter also defines the direction of the cations in the electric field and shows the influence of charge on the electrophoretic mobility. It should be mentioned that the experimental values of the electrophoretic mobilities were obtained at pH 2.5, where most of the species bear a positive charge. The parameter of MO_x is also able to distinguish between the isomers. Comparison of these results with the results of a previous work on alkylpyridines [20] reveals that the descriptor of $(RVDW)^{-1}$ plays some role in electrophoretic mobility. The parameter of distance between the center of mass and center of charge of the molecules (radius of inertia, RI) in the previous work replaces the MO_x parameter in this work. It is noteworthy that radius of inertia was also calculated in this work as a geometric descriptor, but did not appear in the model.

4.2. Neural network analysis

In order to investigate the nonlinear interactions between different parameters in the MLR model, an ANN was developed to predict the electrophoretic mobility of isomeric alkyl- and alkenylpyridines. The ANN was generated using the descriptors appearing in the MLR model as inputs. A 3-6-1 ANN was developed. Fig. 2 shows a plot of the SET and SEP versus the number of iterations, which represents the ''learning curve'' and was used to estimate the extent of training. It can be seen from this figure that while the SET continues to decrease during progress of iteration, the SEP starts to increase after 31,000 iterations. This situation was called overtraining and causes the ANN to be overfitted to the training set and lose its prediction power. Therefore, training of the network is stopped when overtraining begins. The ANN calculated values of the electrophoretic

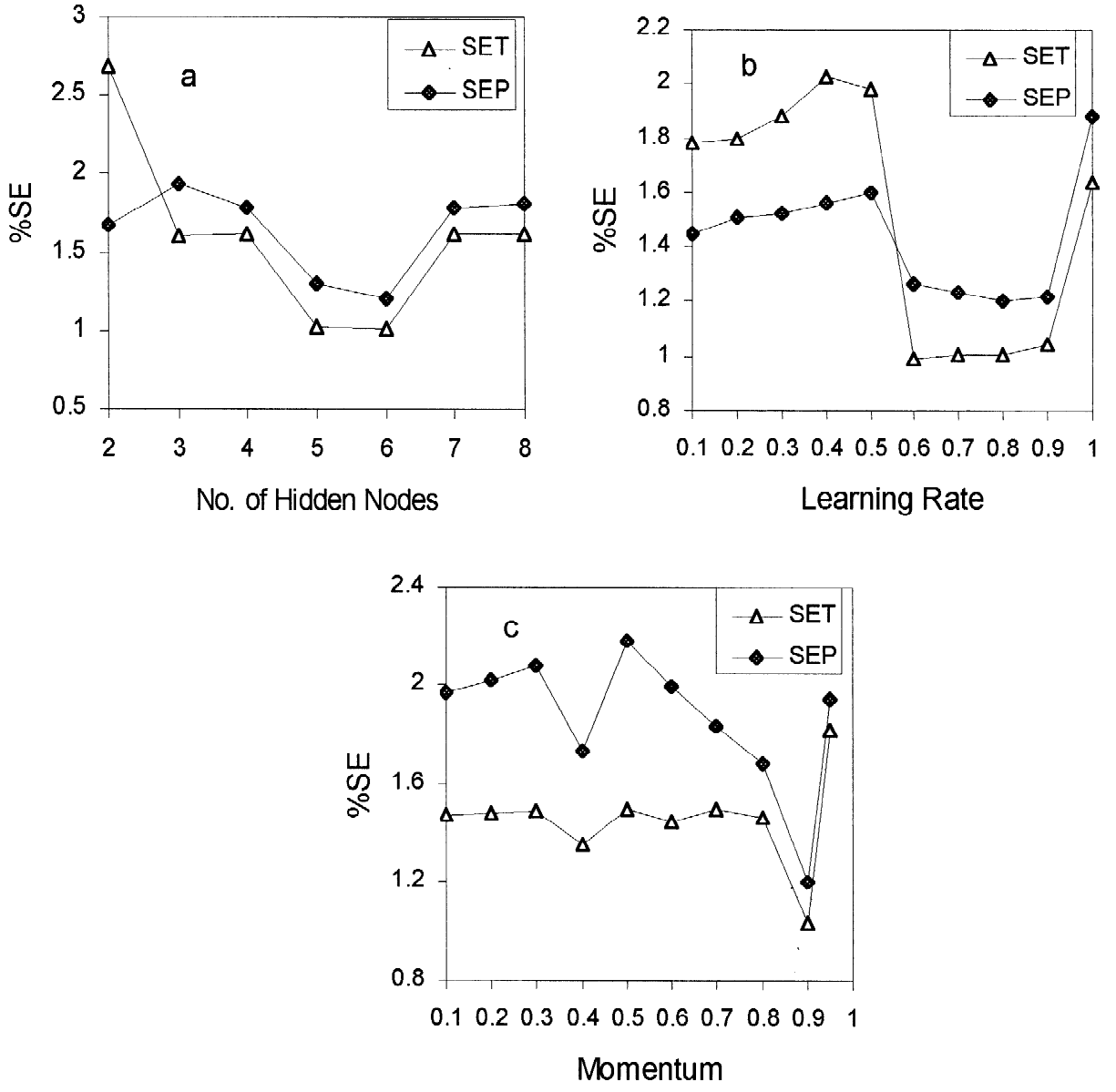

Fig. 1. Values of SET and SEP when overtraining began against the (a) number of nodes in the hidden layer; (b) learning rate; (c) momentum.

mobility for the training and prediction sets are given in Table 1. Comparison of the results obtained using the ANN and MLR methods indicate the superiority of ANN over that of the regression model (Table 4). It can be seen from this table that SET and SEP have been reduced from 6.28 and 5.11% for the MLR model to 1.03 and 1.20% for the ANN model, respectively. The trend of variation of the ANN predicted values of migration are in agreement with the experiment for different isomers. This confirms the validity of the ANN model and indicates that the selection of the MLR descriptors as inputs was suitable. The largest difference between the calculated and experimental values of electrophoretic

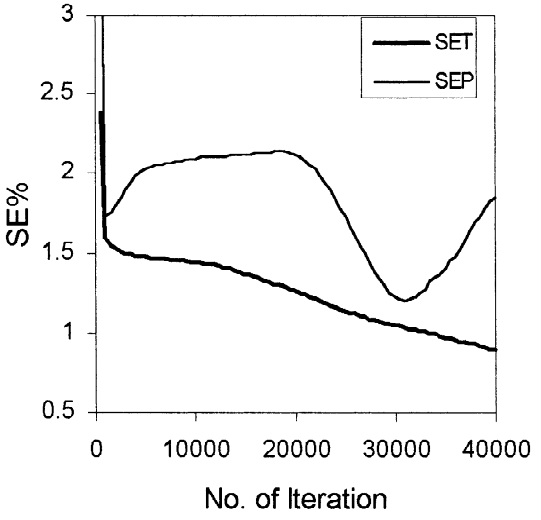

Fig. 2. A typical learning curve.

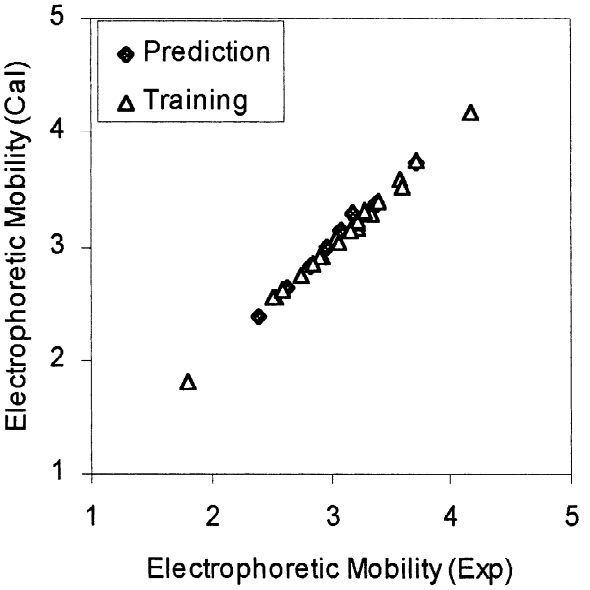

Fig. 3. Plot of calculated electrophoretic mobility against the experimental values.

Table 4
Comparison between the results obtained using the ANN and MLR models

Data set	ANN		MLR	
	R	SE (%)	*R*	SE (%)
Training set	0.998	1.03	0.993	6.28
Prediction set	0.997	1.20	0.991	5.11

mobility (0.092×10^{-4} cm^2 V^{-1} s^{-1}) is due to 2,4-dimethylpyridine. As both the MLR and ANN models of this work and the MLR model in the previous work predict a higher value for the electrophoretic mobility of this molecule, one may conclude that the experimental value for this molecule is underestimated. It is noteworthy that the network has a 3-6-1 architecture with 31 adjustable parameters. On the other hand the training set consists of 22 compounds. Since the data set was small, different prediction and training sets were chosen and the network was trained using these training sets. A set of nine compounds out of 31 molecules was chosen randomly as a prediction set each time and a network was developed using the remaining compounds and then the electrophoretic mobility of nine compounds was predicted by using the ANN model. This procedure was repeated three times and the results are given in Table 5 for the three test sets. In order to show that the data set is randomly divided, the numbers of the molecules for the prediction sets are given in this table. However, the remaining molecules of each set were the corresponding training sets. As can be seen from this table, the results do not depend on the molecules of the prediction set. Fig. 3 shows the plot of the calculated against the experimental electrophoretic mobilities. The resid-

Table 5
Comparison of the SET and SEP of the selected model with the test models obtained using different molecules as prediction set

Model	SET	SEP	No. of molecules in the prediction set[a]
Selected model	0.010	0.012	23, 24, 25, 26, 27, 28, 29, 30, 31
Test model I	0.014	0.017	6, 13, 30, 2, 22, 17, 15, 27, 4
Test model II	0.013	0.015	16, 29, 11, 4, 7, 24, 12, 20, 18
Test model III	0.012	0.012	31, 5, 8, 1, 14, 25, 3, 17, 21

[a] Numbers refer to the number of the compounds given in Table 1. The remaining molecules for each set are due to the corresponding training set.

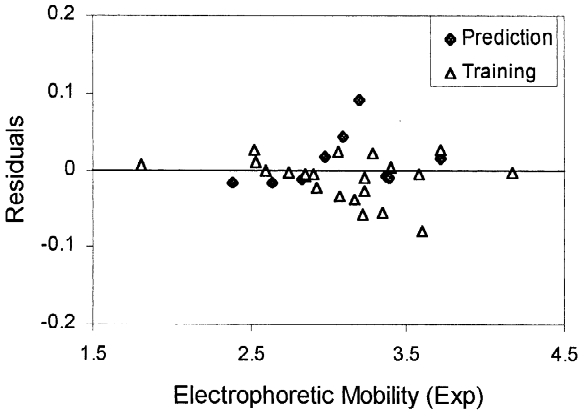

Fig. 4. Plot of residuals versus experimental electrophoretic mobility.

uals of ANN predicted values of mobilities are plotted against the experimental values in Fig. 4. As the calculated residuals are distributed on both sides of zero one may conclude that there is no systematic error in the development of the neural network.

5. Conclusions

Two common methods of MLR and ANN were used to predict the electrophoretic mobility of alkyl- and alkenylpyridines. Both methods seem to be useful, but comparison of these methods shows the superiority of ANN over that of the regression model. Also, the ANN is able to predict the trend of variation in the values of migration for different isomers, while the MLR has lower predictive ability in this respect. The superiority of ANN over that of MLR reveals that the electrophoretic mobility of substituted pyridines shows some nonlinear characteristics. On the other hand, since the descriptors appearing in the MLR model were used as inputs for the ANN, one may conclude that the former method is a suitable technique for choosing the inputs for the neural networks.

References

[1] R. Kaliszan, M. Turowski, A. Bucinsjki, R.A. Hartwick, Quantum Struct. Act. Relat. 14 (1995) 356.
[2] H.R. Liang, H. Vuorela, P. Vuorela, R. Hiltunen, M.L. Riekkola, J. Chromatogr. A 798 (1997) 233.
[3] P. Lukkari, H. Vuorela, M.L. Riekkola, J. Chromatogr. A 652 (1993) 451.
[4] S.Y. Yang, J.G. Bumgarner, L.F.R. Kruk, M.G. Khaledi, J. Chromatogr. A 721 (1996) 323.
[5] N. Majcen, K. Rajer-Kanduc, M. Novic, J. Zupan, Anal. Chem. 67 (1995) 2154.
[6] H. Chan, A. Butler, D.M. Falck, M.S. Freund, Anal. Chem. 69 (1997) 2373.
[7] O. Jimenz, I. Benito, M.L. Marina, Anal. Chim. Acta 353 (1997) 367.
[8] H.J. Metting, P.M.J. Coenegracht, J. Chromatogr. A 728 (1996) 47.
[9] K.L. Peterson, Anal. Chem. 64 (1992) 379.
[10] A.R. Katritzky, E.V. Gordeeva, J. Chem. Inf. Comput. Sci. 33 (1993) 835.
[11] M. Jalali-Heravi, M.H. Fatemi, Anal. Chim. Acta 415 (2000) 95.
[12] M. Jalali-Heravi, M.H. Fatemi, J. Chromatogr. A 897 (2000) 227.
[13] M. Jalali-Heravi, Z. Garkani-Nejad, J. Chromatogr. A 927 (2001) 211.
[14] W.L. Xing, X.W. He, Anal. Chim. Acta 349 (1997) 283.
[15] M.T. Hagan, H.B. Demuth, M. Beal, Neural Network Design, PWS, Boston, 1996.
[16] S. Haykin, Neural Network, Prentice-Hall, Englewood Cliffs, NJ, 1994.
[17] N.K. Bose, P. Liang, Neural Network, Fundamentals, McGraw-Hill, New York, 1996.
[18] D.W. Patterson, Artificial Neural Networks: Theory and Applications, Simon and Schuster, New York, 1996.
[19] J. Zupan, J. Gasteiger, Anal. Chim. Acta 248 (1991) 1.
[20] G.M. Andrew, R.M. Smith, Anal. Chem. 71 (1999) 497.
[21] M. Jalali-Heravi, Z. Garkani-Nejad, J. Chromatogr. 648 (1993) 389.
[22] MOPAC Package, Version 6, US Air Force Academy, Colorado Springs, CO.
[23] Hyperchem, Molecular Modeling System, Hyper Cube, Inc. and Auto Desk, Inc, 1993, Developed by Hyper Cube, Inc.
[24] SPSS/PC, Statistical Package for IBMPC, Quiad software, Ontario, 1986.
[25] T.R. Stouch, P.C. Jurs, J. Chem. Inf. Comput. Sci. 26 (1986) 26.
[26] P.D. Grossman, J.C. Colburn, H.H. Lauer, Anal. Biochem. 179 (1989) 28.
[27] J.T. Edward, D. Waldron-Edward, J. Chromatogr. 20 (1965) 563.